Synthesis, X-ray structural and spectroscopic study of new silyl-substituted triosmium clusters

H.G. Ang, B. Chang, W.L. Kwik and Eunice S.H. Sim

Department of Chemistry, National University of Singapore, Lower Kent Ridge Road, Singapore 0511 (Singapore)

(Received July 7, 1993; in revised form October 27, 1993)

Abstract

The 2-pyridyldimethylsilane, 2-$(CH_3)_2SiHC_5H_4N$**LH** reacts with $[Os_3(\mu\text{-}H)_2(CO)_{10}]$ to afford the novel cluster $[Os_3(\mu\text{-}H)_2(CO)_{10}L_2]$ **1** in which each of the ligands L has been shown from single crystal X-ray diffraction study to bond to one osmium atom through the silicon atom only. In addition, several silyl-substituted triosmium clusters of general formula $[Os_3(\mu\text{-}H)(CO)_{11}\{2\text{-}BrC_6H_4CH_2Si(CH_3)_{2-n}H_n\}]$ (n = 0, **2A**; 1, **2B**; 2, **2C**), $[Os_3(\mu\text{-}H)(CO)_{10}(CH_3CN)\{2\text{-}BrC_6H_4CH_2Si(CH_3)_{2-n}H_n\}]$ (n = 0, **3A**; 1, **3B**) have been synthesized from the reactions of the silane derivatives $BrC_6H_4CH_2Si(CH_3)_{3-m}H_m$ [m = 1, **I**; 2, **II**; 3, **III**] with the activated clusters $[Os_3(CO)_{11}CH_3CN]$ and $[Os_3(CO)_{10}(CH_3CN)_2]$, respectively. The acetonitrile molecule in **3A** is readily substituted by a triphenylphosphine molecule to yield $[Os_3(\mu\text{-}H)(CO)_{10}(Ph_3P)\{2\text{-}BrC_6H_4CH_2Si(CH_3)_2\}]$ (**4**). Reaction of $[Os_3(\mu\text{-}H)_2(CO)_{10}]$ with 2-$BrC_6H_4Si(CH_3)_2H$ affords the cluster $[Os_3(\mu\text{-}H)_3(CO)_9\{2\text{-}BrC_6H_4CH_2Si(CH_3)_2\}]$ (**5**). In the case of **3A** the silane moiety bonds to an osmium atom at a position equatorial to the Os_3 triangle while the acetonitrile molecule takes up an axial position. The molecular structure of **4** contains both the silane and the triphenylphosphine moieties at the terminal, equatorial positions on two separate osmium atoms. The behaviour under high performance liquid chromatography of these clusters has been determined and correlated with the nature of the ligands and with the molecular weights and sizes of the clusters.

Key words: Silyl; Osmium; X-ray diffraction

1. Introduction

We have previously reported the preparation and reactivity towards metal carbonyls of 2-pyridyldimethylsilane [1]. It is of interest to note that only a few X-ray structures have so far been reported for triosmium carbonyl derivatives containing the pyridyl or substituted pyridyl moiety [2]. More recently, we have reported [1] that the phosphinobenzyl- and arylsilanes 2-$Ph_2PC_6H_4CH_2Si(CH_3)_{3-n}H_n$ and 2-$H_n(CH_3)_{3-n}SiC_6H_4CH_2PPh_2$ (n = 1 or 2) act as bidentate ligands in reactions with $[Os_3(CO)_{10}(CH_3CN)_2]$ and $[Os_3(\mu\text{-}H)_2(CO)_{10}]$. As part of our continuing interests in the chemistry of triosmium clusters containing the Os–Si bond, we report below the reactions of triosmium carbonyl clusters with the 2-pyridyldimethylsilane as well as with the *o*-bromobenzyl-, -methyl-, and -dimethylsilanes.

Correspondence to: Dr. H.G. Ang.

0022-328X/94/$7.00
SSDI 0022-328X(93)24268-A

2. Results and discussion

The preparation as well as some spectroscopic properties of **LH** have previously been reported [1].

Ligands **I**, **II** and **III** were synthesized by the Grignard method followed by reduction using excess lithium aluminium hydride [3] in the case of **II** and **III**. These silanes were characterized by IR, ^1H and ^{29}Si NMR spectroscopy [4,5] as given in Table 1.

2.1. Reaction of 2-$(CH_3)_2HSiC_5H_4N$ with $[Os_3(\mu\text{-}H)_2(CO)_{10}]$

The $[Os(\mu\text{-}H)_2(CO)_{10}L_2]$ (**1**) was obtained as the major product from the reaction of 2-$(CH_3)_2SiHC_5H_4N$ **LH** with $[Os_3(\mu\text{-}H)_2(CO)_{10}]$ in cyclohexane for 72 h at room temperature. The carbonyl stretching region of **1** showed absorption peaks at 2086.0w, 2036.0m, 2017.5m, 1994.0s and 1976.0m cm^{-1}, similar in pattern to that of $[Os_3H(CO)_{10}\{Si(OCH_3)_3\}(dppm\text{-}P)]$ and of $[\{Os_3H(CO)_{10}Si(OCH_3)_3\}_2(\mu\text{-}dppe)]$ [6].

TABLE 1. Infrared absorption bands (cm^{-1}) and NMR spectral data in $CDCl_3$ for ligands **I**, **II** and **III**

I	IR	2124vs, 1592m, 1565m, 1467s, 1436s, 1251s, 887vs, 841s, 824s.
	δ_H	0.097(d, CH_3), 2.350(d, CH_2), 4.013(m, SiH), 7.147(m, C_6H_4).
	δ_{Si}	−12.06
II	IR	2141vs, 1592m, 1592m, 1565m, 1467s, 1254s, 897vs, 871s, 825s.
	δ_H	0.111(t, CH_3), 2.378(t, CH_2), 3.872(m, SiH), 7.123(m, C_6H_4).
	δ_{Si}	−32.42
III	IR	2157vs, 1591m, 1561m, 1467s, 1436s, 940vs, 912vs, 860s, 829s.
	δ_H	2.384(q, CH_2), 3.659(t, SiH), 7.125(m, C_6H_4).
	δ_{Si}	−57.67

The ^1H NMR spectrum in $CDCl_3$ showed the presence of bridging hydride at δ −19.605. This is comparable to the bridging hydride of $[Os_3(\mu\text{-H})(CO)_{10}\{Si(OCH_3)_3\}(dppm)]$ and $[(Os_3(\mu\text{-H})\text{-}(CO)_{10}Si(OCH_3)_3\}_2(\mu\text{-dppe})]$ [6]. In addition resonances due to the methyl protons appear as a singlet at δ 0.790 and the pyridyl protons as a multiplet centred at δ 8.05.

2.2. *X-ray crystal structure of $[Os_3(\mu\text{-}H)_2(CO)_{10}\{2\text{-}(CH_3)_2SiC_5H_4N\}]$ (1)*

The molecular structure of **1** is shown in Fig. 1 while the atomic coordinates are given in Table 2 and the relevant bond lengths and angles in Table 3.

The osmium atoms of **1** form a triangle with Os–Os bond lengths of 2.997(4), 2.915(4) and 2.909(2) Å comparable to those of $[Os_3(\mu\text{-H})(CO)_{10}(CH_3CN)(2\text{-Br-}C_6H_4CH_2Si(CH_3)_2\}]$ (**3A**) and $[Os_3(\mu\text{-H})(CO)_{10}\{2\text{-Br-}C_6H_4CH_2Si(CH_3)_2\}(PPh_3)$ (**4**) (below). The longest Os–Os separation is that between Os(1) and Os(2) each of which is bonded to a ligand molecule **L**. The silane molecules assume *cis*-equatorial positions. More interestingly, each of **L** is coordinated through the Si atom only. Moreover, the two pyridine planes are tilted nearly symmetrically above and below the triosmium plane (50.3° and 57.2° from triosmium plane) and are almost perpendicular to each other (95.0°). The Os–Si bonds are 2.434(4) and 2.431(4) Å, which fall within the range for Os–Si bonds of 2.32–2.45 Å observed for triosmium cluster derivatives containing silanes [1,6–

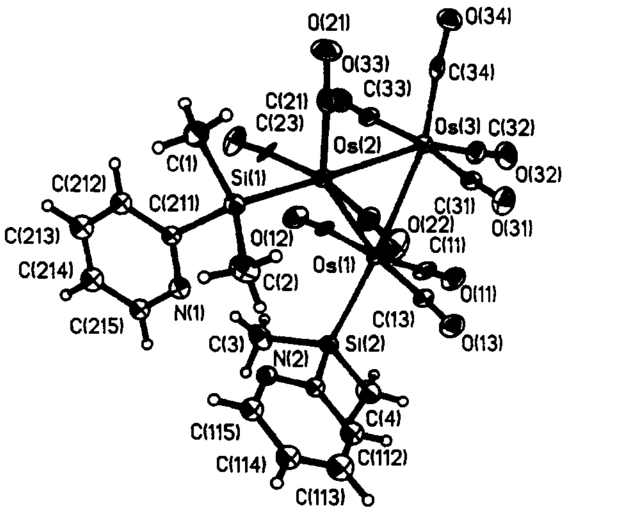

Fig. 1. The molecular structure of $[Os_3(\mu\text{-H})_2(CO)_{10}\{2\text{-}(CH_3)_2\text{-}SiHC_5H_4N\}_2]$ showing the atom labelling scheme.

TABLE 2. Fractional atomic coordinates ($\times 10^4$) and equivalent isotropic coefficients ($Å \times 10^3$) for $Os_3(\mu\text{-H})_2(CO)_{10}[(2\text{-}(CH_3)_2\text{-}SiC_5H_4N)_2]$

	x	y	z	U_{eq} [a]
Os(1)	314(1)	1749(1)	928(1)	32(1)
Os(2)	371(1)	3140(1)	−126(1)	32(1)
Os(3)	−1891(1)	2498(1)	349(1)	39(1)
Si(1)	2200(3)	3705(2)	−625(2)	36(1)
Si(2)	2275(2)	1230(2)	1318(2)	35(1)
N(1)	3964(8)	3226(5)	643(5)	38(3)
N(2)	3880(8)	1761(5)	76(5)	38(3)
C(1)	1961(11)	4666(7)	−1076(9)	59(4)
C(2)	3019(11)	3193(8)	−1504(7)	59(5)
C(3)	3204(11)	1774(7)	2140(7)	59(5)
C(4)	2231(11)	265(7)	1759(9)	67(5)
C(11)	−481(11)	1003(6)	1521(7)	47(4)
C(12)	518(10)	2302(5)	1995(7)	38(3)
C(13)	361(9)	1133(6)	−96(7)	40(3)
C(21)	−546(10)	3887(7)	−676(8)	48(4)
C(22)	464(11)	2572(6)	−1178(8)	47(4)
C(23)	675(10)	3724(5)	925(7)	42(4)
C(31)	−2902(12)	1813(7)	905(8)	54(4)
C(32)	−1823(10)	1919(6)	−705(9)	50(4)
C(33)	−1681(10)	3097(6)	1387(9)	47(4)
C(34)	−2926(10)	3189(6)	−222(8)	51(4)
O(11)	−982(8)	545(5)	1884(6)	67(3)
O(12)	710(8)	2579(5)	2664(5)	61(3)
O(13)	435(9)	753(5)	−700(6)	72(4)
O(21)	−1085(8)	4378(5)	−1001(6)	71(4)
O(22)	582(10)	2247(6)	−1814(6)	77(4)
O(23)	911(9)	4034(5)	1553(5)	67(3)
O(31)	−3544(8)	1419(5)	1227(7)	78(4)
O(32)	−1850(9)	1593(5)	−1363(6)	73(4)
O(33)	−1611(8)	3448(5)	2018(6)	67(3)
O(34)	−3645(7)	3574(5)	−553(6)	62(3)
C(111)	3252(9)	1165(6)	324(6)	36(2)
C(112)	3365(10)	518(7)	−161(7)	52(3)
C(113)	4092(12)	493(8)	−852(9)	67(4)
C(114)	4748(10)	1095(7)	−1077(8)	53(3)
C(115)	4618(10)	1721(6)	−597(7)	47(3)
C(211)	3419(9)	3822(6)	296(6)	35(2)
C(212)	3722(10)	4518(6)	637(7)	46(3)
C(213)	4605(11)	4578(7)	1300(8)	56(3)
C(214)	5155(11)	3960(7)	1641(8)	57(3)
C(215)	4823(10)	3286(6)	1295(7)	44(3)

[a] Equivalent isotropic U defined as one third of the trace of the orthogonalized U_{ij} tensor.

TABLE 3. Selected bond lengths (Å) and bond angles (°) for $[Os_3(\mu\text{-}H)_2(CO)_{10}\{2\text{-}(CH_3)_2SiC_5H_4N\}_2]$ (**1**)

Bond lengths			
Os(1)–Os(2)	2.997(4)	Os(2)–Si(1)	2.431(4)
Os(1)–Os(3)	2.915(4)	Mean Os–C	1.903
Os(2)–Os(3)	2.909(4)	Mean C–O	1.151
Os(1)–Si(2)	2.434(4)	Mean Si–CH_3	1.880
Bond angles			
Os(2)–Os(1)–Os(3)	58.9(1)	Os(1)–Os(2)–Si(1)	123.7(1)
Os(1)–Os(2)–Os(3)	59.1(1)	Os(3)–Os(2)–Si(1)	176.0(1)
Os(1)–Os(3)–Os(2)	62.0(1)	Mean Os–Si–C	114.9
Os(2)–Os(1)–Si(2)	114.5(1)	Mean Os–C–O	176.2
Os(3)–Os(1)–Si(2)	173.5(1)		

10]. The average Os–Si–C bond angle is 114.9°, indicating that the sp^3 hybridization of silicon is well preserved.

Compound **1** contains ten terminally bound carbon monoxide ligands with Os–C and C–O bond lengths falling into the ranges 1.861–1.926 (mean 1.903) Å and 1.137–1.171 (mean 1.154) Å, respectively. These bond lengths are typical of silicon-bonded triosmium clusters which have ranges for Os–C and C–O bond lengths of 1.87–1.93 and 1.13–1.19 Å respectively [1,8–10].

The two bridging hydrides are not located crystallographically but are determined from ^1H NMR which also indicates that the environment of the two hydrides must be similar, as only one bridging hydride peak is observed. A singly hydride-bridged Os–Os bond has been reported to possess bond lengths within the range 3.000–3.155 Å [1,6–10]. An unusually short singly hydride-bridged Os–Os bond of 2.965(1) Å is found in $[Os_3(CO)_9(\mu\text{-}H)\{\mu_3\text{-}\eta^3\text{-}Si(OC_2H_5)_3\}]$ [7]. Thus, it is unlikely that the Os(1)–Os(3) and Os(2)–Os(3) bonds, of lengths 2.915(4) and 2.909(4) Å respectively, are singly bridged in each case by a hydride, implying that the two hydrides must bridge the Os(1)–Os(2) bond.

It should be noted that the prospective coordinating pyridyl N atom is not coordinated. This may be due to the ready cleavage of the extremely weak Si–H bond yielding a reactive unsaturated silicon atom which then coordinates quickly. As excess ligand was used in the preparation, another **L** was coordinated to the other available site before the N atom had a chance to attack the vacant site. The disubstituted structure of **1** through silicon atoms only is unusual as in other triosmium carbonyl derivatives $[(\mu\text{-}H)Os_3(CO)_{10}(2\text{-}YC_5H_4N)]$ (Y = S, NH) [11], the substituted pyridyl moiety has been reported to bond through both pyridyl N and Y.

2.3. *Reactions of I, II and III with $[Os_3(CO)_{11}(CH_3CN)]$*

The three products **2A**, **2B** and **2C** obtained from reactions of **I**, **II** and **III**, respectively, with $[Os_3(CO)_{11}(CH_3CN)]$, display carbonyl stretching frequencies remarkably similar to those of $[Os_3(\mu\text{-}H)(CO)_{11}(Si(C_2H_5)_3)]$ [12]. Due to these strong absorptions, the Si–H stretching frequencies for **2B** and **2C** were masked.

The $[Os_3(\mu\text{-}H)(CO)_{11}L']$ (L′H = **I**, **II** and **III**) formulations are supported by the high field resonances at δ − 18.570, − 18.760 and − 18.930 ppm, typical of bridging hydrides [13]. Those of $[Os_3(\mu\text{-}H)(CO)_{11}(SiR_3)]$ ($R_3 = (OCH_3)_3$, $(OC_2H_5)_3$, $(C_2H_5)_3$, HPh_2) have been reported [12] to lie between δ − 18.32 and − 18.76. Interestingly enough, the bridging hydride in **2A**, **2B** and **2C** shifts downfield as the Si–H is substituted by $-CH_3$, just like that observed for the Si–H resonances of **I**, **II** and **III**.

2.4. *Reactions of I, II and III with $[Os_3(CO)_{10}(CH_3CN)_2]$*

Products **3A** and **3B** obtained from reactions of **I** and **II** respectively with $[Os_3(CO)_{10}(CH_3CN)_2]$ are sufficiently stable to allow for spectroscopic study. Crystals of **3A** of X-ray diffraction quality were obtained by slow crystallization from a hexane solution. **3A** and **3B** display C–O stretching vibrations similar to those reported [6,7] for $[Os_3(\mu\text{-}H)(CO)_{10}(CH_3CN)(SiR_3)]$ ($R_3 = (OCH_3)_3$, $(OC_2H_5)_3$, $(C_2H_5)_3$ or HPh_2). The ^1H NMR of **3A** and **3B** are consistent with the formulation $[Os_3(\mu\text{-}H)(CO)_{10}(CH_3CN)L']$ as these contain resonances at δ 2.623 and 2.762 respectively, due to methyl protons of CH_3CN as well as high-field resonances at δ − 16.233 and − 16.396 respectively due to the bridging hydrides. Those of $[Os_3(\mu\text{-}H)(CO)_{10}(CH_3CN)(SiR_3)]$ [$R_3 = (OCH_3)_3$, $(OC_2H_5)_3$, $(C_2H_5)_3$ or HPh_2] lie in a narrow range of − 16.09 to − 16.56 ppm [6,7].

2.5. *X-ray crystal structure of $[Os_3(\mu\text{-}H)(CO)_{10}(CH_3CN)(2\text{-}BrC_6H_4CH_2Si(CH_3)_2)]$ (3A)*

The molecular structure of **3A** is shown in Fig. 2 while the atomic coordinates are given in Table 4 and

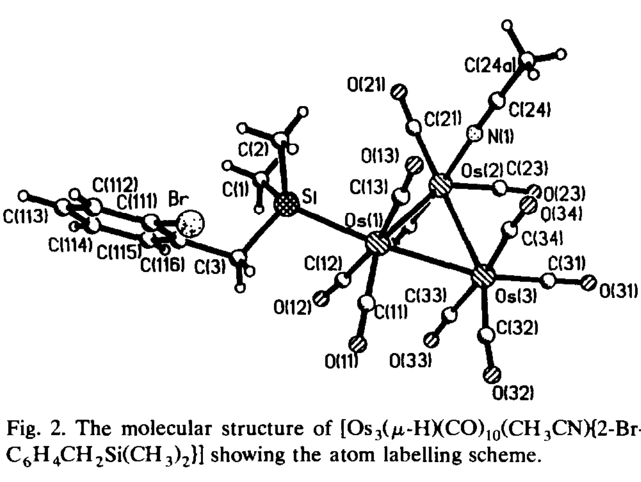

Fig. 2. The molecular structure of $[Os_3(\mu\text{-}H)(CO)_{10}(CH_3CN)\{2\text{-}BrC_6H_4CH_2Si(CH_3)_2\}]$ showing the atom labelling scheme.

TABLE 4. Fractional atomic coordinates ($\times 10^4$) and equivalent isotropic coefficients ($Å \times 10^3$) for $[Os_3(\mu\text{-}H)(CO)_{10}(CH_3CN)(2\text{-}BrC_6H_4CH_2Si(CH_3)_2)]$ (3A)

	x	y	z	U_{eq} [a]
Os(1)	4006(1)	2324(1)	6132(1)	28(1)
Os(2)	3346(1)	1678(1)	8218(1)	29(1)
Os(3)	6096(1)	1886(1)	7936(1)	31(1)
Si	2037(5)	2606(4)	4728(3)	34(2)
C(11)	5250(21)	2711(18)	5280(13)	44(7)
C(12)	4089(23)	4011(17)	6554(15)	49(8)
C(13)	3593(18)	676(16)	5509(11)	31(6)
C(21)	1523(25)	1483(22)	8339(15)	59(9)
C(22)	3553(22)	3362(22)	8686(14)	52(8)
C(23)	4157(18)	1380(15)	9617(13)	39(6)
N(1)	2993(14)	−187(14)	7685(11)	36(5)
C(31)	7041(22)	1499(17)	9287(15)	47(7)
C(32)	7451(16)	2108(17)	7172(14)	40(6)
C(33)	6321(22)	3584(21)	8392(13)	51(8)
C(34)	5638(19)	223(18)	7323(14)	42(7)
O(11)	6035(16)	3030(14)	4782(11)	64(6)
O(12)	4082(19)	5021(11)	6767(12)	70(7)
O(13)	3311(18)	−299(11)	5117(10)	64(7)
O(21)	415(15)	1347(17)	8468(13)	73(7)
O(22)	3627(18)	4330(13)	8983(12)	66(7)
O(23)	4689(16)	1261(14)	10500(9)	59(6)
C(24)	2775(19)	−1222(17)	7501(14)	41(7)
C(24A)	2550(28)	−2489(18)	7284(18)	66(10)
O(31)	7639(16)	1217(15)	10098(11)	74(7)
O(32)	8367(16)	2208(14)	6735(12)	63(6)
O(33)	6527(16)	4624(13)	8681(12)	64(6)
O(34)	5495(15)	−743(12)	6958(11)	50(5)
C(1)	826(27)	3396(22)	5308(18)	73(11)
C(2)	939(24)	1204(19)	3953(18)	66(9)
C(3)	2622(21)	3576(17)	3702(13)	43(7)
Br	1995(4)	1940(3)	1424(2)	114(2)
C(111)	1109(23)	3210(18)	1789(15)	51(5)
C(112)	117(21)	3474(17)	972(14)	45(4)
C(113)	−568(23)	4429(18)	1124(16)	54(5)
C(114)	−156(23)	5081(19)	2144(15)	54(5)
C(115)	857(20)	4791(17)	2976(14)	45(4)
C(116)	1508(20)	3852(16)	2810(13)	41(4)

[a] Equivalent isotropic U defined as one third of the trace of the orthogonalized U_{ij} tensor.

the relevant bond lengths and angles in Table 5. The Os–Os bond lengths of 2.991(1), 2.892(1) and 2.886(2) Å are significantly longer than the average bond length of 2.877(3) Å in $[Os_3(CO)_{12}]$ [14] and those of $[Os_3(CO)_{10}(CH_3CN)_2]$ (2.842(2), 2.875(2) and 2.979(2) Å) [15] but comparable to those of $[Os_3(\mu\text{-}H)(CO)_{10}(CH_3CN)(Si(OC_2H_5)_3)]$ [7] (2.894(3), 3.008(2), 2.888(2) Å). As would be expected the longest Os–Os bond corresponds to that between the two osmium centres bonded to the silane and the CH_3CN respectively. Furthermore the bridging hydride as determined from ^1H NMR would have enhanced the lengthening effect [16].

The acetonitrile ligand occupies an axial site and is nearly linear, with the Os(2)–N–C bond angle being 172.8(15)°. The bonds Os(2)–N (2.11(2) Å) and C–N (1.15(2) Å) are comparable to the corresponding ones in $[Os_3(CO)_{11}(CH_3CN)]$ and $[Os_3(CO)_{10}(CH_3CN)_2]$.

The bulky silane molecule assumes an equatorial position. The Os–Si bond of 2.452(5) Å lies in the range reported [6–10,17] for triosmium cluster derivatives (2.367(13)–2.455(2) Å). Finally the Si–C bond lengths range from 1.868(20) to 1.898(19) Å. The Os(1)–Si–C bond angles being 111.8(7)°, 116.4(7)° and 110.0(6)° (mean 112.8°) suggest that the sp^3 hybridization of Si is preserved.

The Os–CO bond lengths range from 1.86(2) to 1.93(2) Å. The C–O bond lengths lie in the range 1.11(3) to 1.19(3) Å. As expected, the shortest C–O bond is that opposite CH_3CN on Os(2). All the carbonyls are terminal and linear as the Os–C–O angles range from 173.44(17)° to 177.9(13)°.

2.6. Reaction of 3A with $P(C_6H_5)_3$

Reaction of **3A** with $P(C_6H_5)_3$ resulted in the substitution of CH_3CN to afford **4**, which, on recrystallization from CH_2Cl_2/hexane, yielded diffraction quality crystals.

The carbonyl stretching frequencies of **4** comprise six distinctive peaks at 2104w, 2060m, 2038m, 2019s, 2000m and 1985ms cm^{-1} similar to those of $[Os_3(\mu\text{-}H)(CO)_{10}\{Si(OCH_3)_3\}(dppe)]$ [6]. Moreover it is noted that marked differences in the carbonyl stretching frequencies existed between **3A** and **4**, suggesting different spatial arrangements of the CO groups in these two molecules.

The presence of a bridging hydride in **4** is determined from the high field resonance in the ^1H NMR at $\delta - 18.946$. Those of $[Os_3(\mu\text{-}H)(CO)_{10}(SiR_3)(dppm)]$ and $[Os_3(\mu\text{-}H)(CO)_{10}(SiR_3)(dppe)]$ [$R_3 = (OCH_3)_3$, $(OC_2H_5)_3$] were observed [6] at $\delta - 19.01$ and $\delta - 19.32$ respectively.

TABLE 5. Relevant bond lengths (Å) and angles (°) for $[Os_3(\mu\text{-}H)(CO)_{10}(CH_3CN)(2\text{-}BrC_6H_4SiH_2Si(CH_3)_2)]$ (3A)

Bond lengths			
Os(1)–Os(2)	2.991(1)	Os(2)–N	2.113(16)
Os(1)–Os(3)	2.892(1)	Mean Os–CO	1.90
Os(2)–Os(3)	2.886(2)	Mean C–O	1.16
Os(1)–Si	2.452(5)	Mean Si–C	1.88
Bond angles			
Os(1)–Os(2)–Os(3)	58.9(1)	Os(2)–Os(1)–Si	114.5(1)
Os(2)–Os(1)–Os(3)	58.7(1)	Os(3)–Os(1)–Si	173.1(1)
Os(1)–Os(3)–Os(2)	62.4(1)	Mean Os(1)–Si–C	112.8
Os(1)–Os(2)–N	91.6(4)	Mean Si–Os(1)–C	87.4
Os(2)–N–C	172.8(15)	Mean Os–C–O	176.2
Os(3)–Os(2)–N	90.1(4)		

2.7. X-ray crystal structure of $[Os_3(\mu\text{-}H)(CO)_{10}\{2\text{-}Br\text{-}C_6H_4CH_2Si(CH_3)_2\}(PPh_3)]$ (4)

The molecular structure of **4** is shown in Fig. 3, the atomic coordinates are given in Table 6 and the relevant bond lengths and angles in Table 7.

The Os–Os bond lengths in the triangular metal framework of **4** are 2.888(2), 2.921(1) and 3.031(2) Å. As in **3A**, the longest Os–Os bond is that between the two osmium atoms bearing the silane and the phosphine, and bridged by the hydride. However, this Os–Os bond is longer in **4** (3.031(2) Å) than that in **3A** (2.991(1) Å). This may, in part, be due to the presence in equatorial *cis*-positions of the PPh_3 and the substituted silane in **4**.

The Os–Si bond length of 2.463(9) Å is somewhat longer than those reported [6–10,17]. The Os–P bond length of **4** (2.367(6) Å), on the other hand, is comparable to that in $[Os_3(\mu\text{-}H)(CO)_{10}\{Si(OC_2H_5)_3\}(dppe)]$ (2.362(3) Å).

The Si–C bonds range between 1.89(4) and 1.97(3) Å, and the Os–Si–C angles (mean 112.8°) indicate that the sp^3 hybridization of silicon is preserved. For the P–C bond lengths, the mean value is 1.81 Å, and the mean Os–P–C bond angle is 114.7°.

The Os–CO bond lengths range from 1.83(3) to 1.99(3) (mean 1.90) Å. The C–O bond lengths range from 1.08(3) to 1.19(4) (mean 1.16) Å. All the carbonyls are terminal and linear, the Os–C–O bond angles ranging from 174(3)° to 179(5)° (mean 176.2°).

2.8. Reactions of I, II and III with $[Os_3(\mu\text{-}H)_2(CO)_{10}]$

The reactions of **II** and **III** with $[Os_3(\mu\text{-}H)_2(CO)_{10}]$ yielded highly unstable products. However, a reasonably stable product which is most likely $[Os_3(\mu\text{-}H)_3(CO)_9\{2\text{-}BrC_6H_4Si(CH_3)_2\}]$ (**5**), was obtained from that of **I**. A similar product was reported by Willis *et*

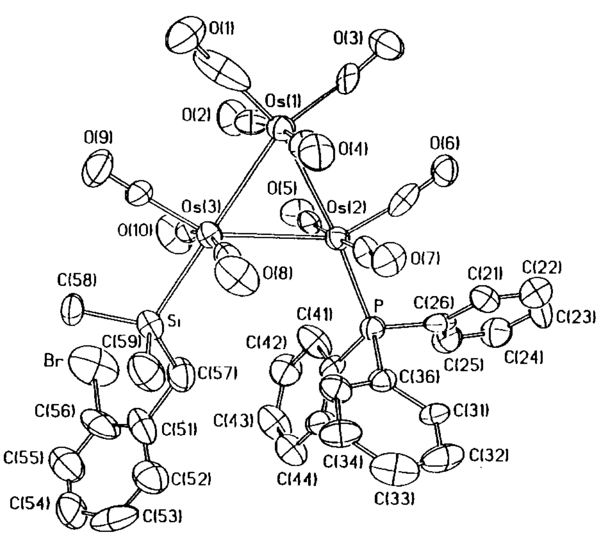

Fig. 3. The molecular structure of $[Os_3(\mu\text{-}H)(CO)_{10}(PPh_3)\{2\text{-}Br\text{-}C_6H_4CH_2Si(CH_3)_2\}]$ showing the atom labelling scheme.

TABLE 6. Fractional atomic coordinates ($\times 10^4$) and equivalent isotropic coefficients (Å $\times 10^3$) for $[Os_3(\mu\text{-}H)(CO)_{10}(PPh_3)\{2\text{-}BrC_6H_4CH_2Si(CH_3)_2\}]$

	x	y	z	U_{eq} [a]
Os(1)	165.0(10)	2617.5(8)	265.1(8)	64.2(2)
Os(2)	1680.4(9)	1016.5(8)	1273.2(7)	56.3(4)
Os(3)	1047.5(10)	2998.1(8)	2031.7(8)	63.4(4)
Br	236(5)	2482(6)	6046(4)	193(4)
P	3010(6)	−139(5)	2163(5)	60(3)
Si	1821(7)	3309(6)	3534(6)	73(3)
O(1)	−1273(20)	4585(17)	−232(18)	125(12)
O(2)	−1847(18)	2144(17)	1508(15)	105(10)
O(3)	−346(21)	1545(15)	−1441(15)	103(10)
O(4)	2208(18)	3282(15)	−706(15)	96(9)
O(5)	−415(15)	418(15)	2341(14)	86(9)
O(6)	1373(16)	−230(12)	−288(14)	82(8)
O(7)	3646(16)	1546(15)	113(14)	88(9)
O(8)	3212(19)	3655(19)	1150(16)	116(12)
O(9)	−256(20)	5049(15)	1923(17)	115(11)
O(10)	−706(20)	2317(20)	3433(15)	126(13)
C(1)	−740(37)	3844(33)	−50(23)	152(24)
C(2)	−1095(32)	2290(23)	1052(19)	109(16)
C(3)	−108(23)	1929(14)	−779(18)	66(10)
C(4)	1487(21)	3001(19)	−346(19)	69(11)
C(5)	344(24)	657(18)	1981(20)	76(11)
C(6)	1537(19)	233(16)	342(21)	72(11)
C(7)	2940(22)	1396(19)	548(16)	64(10)
C(8)	2414(28)	3401(21)	1437(20)	86(13)
C(9)	207(25)	4298(19)	1971(21)	80(12)
C(10)	−89(22)	2582(23)	2865(21)	85(13)
C(21)	3557(16)	−1397(16)	795(13)	80(13)
C(22)	3699	−2293	415	116(19)
C(23)	3485	−3095	977	144(24)
C(24)	3129	−3002	1919	100(16)
C(25)	2987	−2106	2298	91(14)
C(26)	3201	−1303	1736	76(12)
C(31)	5386(15)	−546(11)	1968(12)	66(10)
C(32)	6457	−308	1972	111(18)
C(33)	6561	627	2143	105(17)
C(34)	5594	1324	2310	92(14)
C(35)	4523	1087	2306	74(12)
C(36)	4419	152	2135	60(10)
C(41)	1684(14)	−531(15)	3765(13)	103(16)
C(42)	1487	−696	4735	110(17)
C(43)	2341	−686	5370	106(17)
C(44)	3392	−511	5036	94(15)
C(45)	3589	−346	4067	81(12)
C(46)	2735	−356	3432	65(10)
C(51)	2528(33)	2355(21)	5352(21)	103(16)
C(52)	3682(36)	2325(28)	5483(26)	115(19)
C(53)	3958(31)	2579(28)	6281(35)	138(22)
C(54)	3106(43)	2817(30)	7017(26)	141(22)
C(55)	2023(45)	2787(31)	6922(31)	137(23)
C(56)	1730(40)	2568(29)	6115(24)	132(21)
C(57)	2150(31)	2128(22)	4381(22)	100(15)
C(58)	816(26)	4260(20)	4166(21)	91(13)
C(59)	3178(28)	3773(28)	3392(25)	121(19)

[a] Equivalent isotropic U defined as one third of the trace of the orthogonalized U_{ij} tensor.

TABLE 7. Relevant bond lengths (Å) and angles (°) for $[Os_3(\mu\text{-}H)(CO)_{10}(PPh_3)\{2\text{-}BrC_6H_4CH_2Si(CH_3)_2\}]$ (4)

Bond lengths			
Os(1)–Os(2)	2.921(1)	Mean Os–CO	1.90
Os(1)–Os(3)	2.888(2)	Mean C–O	1.16
Os(2)–Os(3)	3.031(2)	Mean Si–C	1.88
Os(3)–Si	2.463(9)	Mean P–C	1.81
Os(2)–P	2.367(6)		
Bond angles			
Os(1)–Os(2)–Os(3)	58.0(1)	Os(1)–Os(3)–Si	179.3(2)
Os(2)–Os(1)–Os(3)	62.9(1)	Os(2)–Os(3)–Si	120.3
Os(1)–Os(3)–Os(2)	59.1(1)	Mean Os(1)–Si–C	112.8
Os(1)–Os(2)–P	173.1(2)	Mean Os(2)–P–C	114.7
Os(3)–Os(2)–P	115.9(2)	Mean Si–Os(1)–C	87.4
Os(2)–P–C(26)	112.3(7)	Mean Os–CO	176.2

al. [9] after reaction of $[Os_3(\mu\text{-}H)_2(CO)_{10}]$ with Ph_3SiH. The X-ray structures of $[Os_3(\mu\text{-}H)_3(CO)_9(SiPh_3)]$ [9] and of $[HOs_3(\mu\text{-}H)_2(CO)_{10}(SiHPh_2)]$ [10] have been determined. The compound **5** was characterized by ν(CO) at *ca.* 2128mw, 2079s, 2047s, 2034vs, 2025m, 2008s and 1970m cm^{-1}, comparable to those of $[Os_3(\mu\text{-}H)_3(CO)_9(SiPh_3)]$.

However, the ^1H NMR spectra of **5** are somewhat more complex. Thus at room temperature only a single resonance was observed at δ − 15.840. At −51°C, three other high field resonances at δ − 12.906, −12.604 and −8.239 of equal intensities were observed. In the case of $[Os_3(\mu\text{-}H)_3(CO)_9(SiPh_3)]$ [9], three equally intense high field resonances at δ − 12.42, −12.29 and −8.58 have been attributed to the presence of three bridging hydrides. Due to the unsaturated nature of **5** and of $[Os_3(\mu\text{-}H)_3(CO)_9(SiPh_3)]$, the chemical shifts of these bridging hydrides are found at lower fields than usual.

2.9. HPLC separation of $[Os_3(CO)_{10}(CH_3CN)_2]$, $[Os_3(CO)_{11}CH_3CN)]$, $[Os_3(\mu\text{-}H)(CO)]_{11}\{2\text{-}BrC_6H_4CH_2Si(CH_3)_2\}]$, $[Os_3(\mu\text{-}H)(CO)_{10}(CH_3CN)\{2\text{-}BrC_6H_4CH_2Si(CH_3)_2\}]$ and $[Os_3(\mu\text{-}H)(CO)_{10}\{P(C_6H_5)_3\}\{2\text{-}BrC_6H_4CH_2Si(CH_3)_2\}]$

Complete separation of the above clusters was achieved under reversed-phase conditions, with the mobile phase being 100% acetonitrile at a flow rate of 0.5 ml/min. The chromatogram is displayed in Fig. 4. The retention times (t), area/height ratios (Ar/Ht), capacity factors (k') and number of theoretical plates (N) of the five clusters are given in Table 8.

The k' values range between 1.5 and 8.5, within the optimum range of $1 < k' < 20$ [18]. The N value of 8500 obtained for $[Os_3(CO)_{11}(CH_3CN)]$ is low in comparison with the value 12500 evaluated using standard equations for a well-packed column of the given specifications [19]. The other four N values are comparable to the expected values. The low value obtained may be

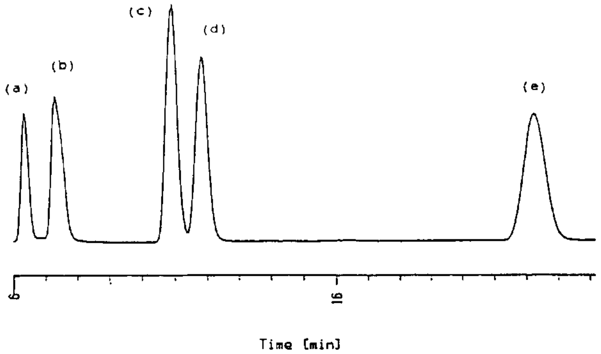

Fig. 4. Reversed phase HPLC chromatogram for the following clusters. From left: (a) $Os_3(CO)_{10}(CH_3CN)_2$; (b) $Os_3(CO)_{11}(CH_3CN)$; (c) $Os_3(\mu\text{-}H)(CO)_{10}(CH_3CN)[2\text{-}BrC_6H_4CH_2Si(CH_3)_2]$; (d) $Os_3(\mu\text{-}H)(CO)_{11}[2\text{-}BrC_6H_4CH_2Si(CH_3)_2]$; (e) $Os_3(\mu\text{-}H)(CO)_{10}[P(C_6H_5)_3][2\text{-}BrC_6H_4CH_2Si(CH_3)_2]$. Mobile phase is 100% acetonitrile; column is LiChrospher 100 CH-18/2, 250×4 mm, 10 μm; flow rate = 0.5 ml min^{-1}.

due to the inefficiency of the column and of the mobile phase in separating this particular compound.

The clusters $[Os_3(CO)_{10}(CH_3CN)_2]$ and $[Os_3(CO)_{11}(CH_3CN)]$ are eluted out first as they are of lower molecular weights than the three clusters of the general formula $[Os_3(\mu\text{-}H)(CO)_{10}(L)\{2\text{-}BrC_6H_4CH_2Si(CH_3)_2\}]$ [L = CO (**2A**), CH_3CN (**3A**), $P(C_6H_5)_3$ (**4**)]. The order of elution for the clusters $[Os_3(CO)_{10}(CH_3CN)_2]$ and $[Os_3(CO)_{11}(CH_3CN)]$ has been previously observed [20–22] and is in agreement with their relative polarities [23]. Of the three clusters **2A**, **3A** and **4** the latter has the longest retention time. The retardation of clusters containing triarylphosphine ligands has been reported [24–26] for both normal- and reversed-phase separations of derivatives of $[(Cp)NiOs_3(\mu\text{-}H)_3(CO)_8L]$ [Cp = cyclopentadienyl, L = CO, PPh_2H, Ph and $P(o\text{-}tolyl)_3$] and also for the series of clusters $[Os_3(CO)_{12-n}\{P(C_6F_5)_n\}]$ (n = 0–2).

The retention times of compounds of the former series of compounds have been correlated with the varying degrees of steric hindrance [25], while those of the latter series increase with increasing number of

TABLE 8. Chromatographic data for clusters of series 1

Cluster	t_R (min)	V_R (ml)	Ar/Ht	k'	N
(a)	6.07	3.03	0.272	1.674	12516
(b)	7.02	3.51	0.387	2.093	8270
(c)	10.62	5.31	0.406	3.678	17196
(d)	11.55	5.77	0.452	4.088	16411
(e)	21.95	10.97	0.811	8.670	18411

(a) $[Os_3(CO)_{10}(CH_3CN)_2]$; (b) $[Os_3(CO)_{11}(CH_3CN)]$; (c) $[Os_3(\mu\text{-}H)(CO)_{10}(CH_3CN)\{2\text{-}BrC_6H_4CH_2Si(CH_3)_2\}]$ (**3A**); (d) $[Os_3(\mu\text{-}H)(CO)_{11}\{2\text{-}BrC_6H_4CH_2Si(CH_3)_2\}]$ (**2A**); (e) $[Os_3(\mu\text{-}H)(CO)_{10}\{P(C_6H_5)_3\}\{2\text{-}BrC_6H_4CH_2Si(CH_3)_2\}]$ (**4**).

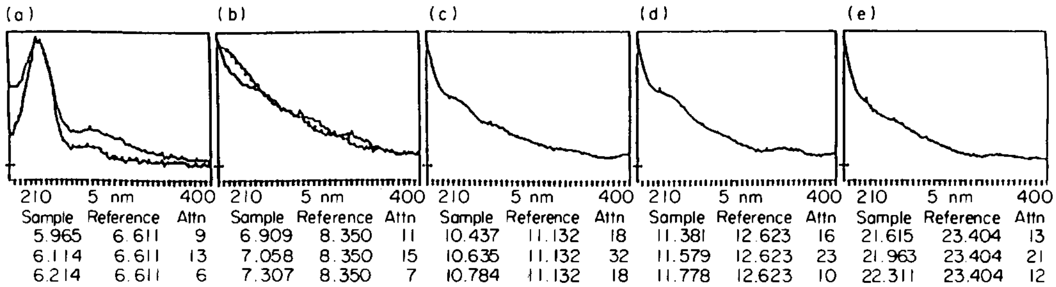

Fig. 5. UV absorption spectra (211–401 nm) for the following clusters between the time intervals, in minutes, shown within brackets, using the photodiode array detector. From left: (a) $Os_3(CO)_{10}(CH_3CN)_2$ (5.99–6.21); (b) $Os_3(CO)_{11}(CH_3CN)$ (6.91–7.31); (c) $Os_3(\mu\text{-}H)(CO)_{10}(CH_3CN)[2\text{-}BrC_6H_4CH_2Si(CH_3)_2]$ (10.44–10.78); (d) $Os_3(\mu\text{-}H)(CO)_{11}[2\text{-}BrC_6H_4CH_2Si(CH_3)_2]$ (11.38–11.78); (e) $Os_3(\mu\text{-}H)(CO)_{10}[P(C_6H_5)_3][2\text{-}BrC_6H_4CH_2Si(CH_3)_2]$ (21.62–22.31). Mobile phase is 100% acetonitrile; column is LiChrospher 100 CH-18/2, 250 × 4 mm, 10 μm; flow rate = 0.5 ml min^{-1}.

phenyl groups [22]. The retention of **4** on the reversed-phase column is most likely due to its large molecular weight and the steric hindrance of its bulky substituent groups.

The elution order of **3A** and **2A** follows that of $[Os_3(CO)_{10}(CH_3CN)_2]$ and $[Os_3(CO)_{11}(CH_3CN)]$ *i.e.* **3A** elutes before **2A**. Again, the relative polarities and hence the relative solubilities of these clusters in the mobile phase appear to be the dominant factor in determining the elution order. The separation of clusters **2A**, **3A** and **4** has illustrated that a change in the ligand **L** in clusters of the general formula $[Os_3(\mu\text{-}H)(CO)_{10}(L)\{o\text{-}BrC_6H_4CH_2Si(CH_3)_2\}]$ [L = CO, CH_3CN, $P(C_6H_5)_3$] strongly influences the retention behaviour in reversed-phase HPLC, thus allowing effective separations of these clusters.

The spectral overlay plots are displayed in Fig. 5 while the ratio plot of the signals at 230 and 254 nm is given in Fig. 6. These plots show that the peaks corresponding to the compounds **3A**, **2A** and **4** are pure, as they are characterized by well-matched spectral overlays and fairly constant ratio plots. However, the peaks corresponding to (a) $[Os_3(CO)_{10}(CH_3CN)_2]$ and (b) $[Os_3(CO)_{11}(CH_3CN)]$ are characterized by ill-matched spectral overlays and varying ratio plots. These may be due to the presence of trace amounts of $[Os_3(CO)_{12}]$,

TABLE 9. Crystallographic data for **1**, **3A** and **4**

	1	**3A**	**4**
Formula	$C_{24}H_{20}N_2O_{10}Os_3Si_2$	$C_{21}H_{15}NO_{10}BrOs_3Si$	$C_{37}H_{27}O_{10}BrOs_3PSi$
Formula weight	1123.2	1119.9	1340.9
Crystal system	Monoclinic	Triclinic	Triclinic
Space group	$P2_1/n$	$P\bar{1}$	$P\bar{1}$
a (Å)	11.182(14)	10.213(2)	12.030(3)
b (Å)	18.086(8)	11.254(5)	14.155(4)
c (Å)	15.213(16)	12.735(1)	14.184(4)
α (°)		93.880(2)	85.35(2)
β (°)	92.53(10)	102.850(4)	87.86(4)
γ (°)		98.640(3)	78.55(2)
V (Å^3)	3074(5)	1403.1(7)	2359.0(1)
Z	4	2	2
$\rho_{(calc)}$ (g cm^{-3})	2.427	2.651	1.888
μ (cm^{-1})	125.03	150.74	90.13
Total reflections	5859	5235	5576
Unique reflections	5370	4937	4412
Observed reflections [a]	4037	3507	2527
No. of variables	370	334	478
R (obsd. data)	0.0346	0.0480	0.0694
R_w (obsd. data)	0.0429	0.0605	0.0698
Goodness of fit	1.01	1.17	1.50

[a] $F_o \geq 5\sigma\ (F_o)$.

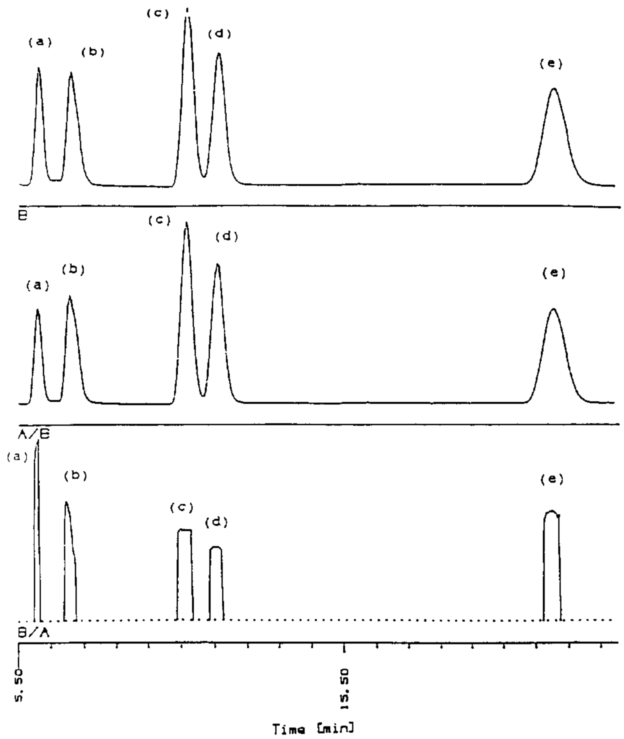

Fig. 6. Ratio plots of signals at 230 nm to that at 254 nm, for the following clusters. From left: (a) $Os_3(CO)_{10}(CH_3CN)_2$; (b) $Os_3(CO)_{11}(CH_3CN)$; (c) $Os_3(\mu\text{-}H)(CO)_{10}(CH_3CN)[2\text{-}BrC_6H_4CH_2Si(CH_3)_2]$; (d) $Os_3(\mu\text{-}H)(CO)_{11}[2\text{-}BrC_6H_4CH_2Si(CH_3)_2]$; (e) $Os_3(\mu\text{-}H)(CO)_{10}[P(C_6H_5)_3][2\text{-}BrC_6H_4CH_2Si(CH_3)_2]$. Mobile phase is 100% acetonitrile; column is LiChrospher 100 CH-18/2, 250×4 mm, 10 μm; flow rate = 0.5 ml min^{-1}.

as it has been found that the mono- and bis-acetonitrile complexes invariably contain small amounts of $[Os_3(CO)_{12}]$ which may have eluted out together with these two activated clusters.

3. Experimental details

The reactions described above were carried out in evacuated reaction tubes. All solvents were dried over appropriate drying agents and distilled prior to use. Infrared spectra were recorded on a Perkin-Elmer model 983G spectrophotometer, ^1H, ^{31}P and ^{29}Si NMR spectra on a JEOL FX-90Q FT instrument using $SiMe_4$ (^1H and ^{29}Si) or H_3PO_4(^{31}P) as references. The products of the reactions were separated by thin-layer chromatography on 20 × 20 cm glass plate coated with 0.5 mm of Merck Kieselgel 60GF, using mixtures of dichloromethane and hexane in various proportions as eluants.

3.1. X-ray structural determination

Crystal data and details of measurements for complexes **1**, **3A** and **4** are reported in Table 9. Diffraction intensities were collected at 298 K on a Siemens R3m/V X-ray diffractometer with graphite-monochromatized Mo Kα radiation (λ = 0.71069 Å), scan range $3.5 < 2\theta < 50.0$ for **1**, 1.2°, $3.0 < 2\theta < 50.0°$, for **3A**, $4.0 < 2\theta < 50.0°$ for **4**. Indices $+h$, $+k$ and $\pm l$ for **1**, $+h$, $\pm k$, $\pm l$ for **3A** and $\pm h$, $\pm k$, $+l$ for **4**. All computations were carried out on a Micro VAX 2000 computer using the SHELXTL PLUS program package [27]. The structures were solved by direct methods for the osmium atoms, and Fourier difference techniques for the remaining non-hydrogen atoms. Full-matrix, least-squares refinement with all non-hydrogen atoms being refined anisotropically and hydrogen atoms in calculated position. An empirical (ψ-scan) correction was performed in each case.

3.2. Reaction of 2-$(CH_3)_2SiHC_5H_4N$ with $[Os_3(\mu\text{-}H)_2(CO)_{10}]$

The $[Os_3(\mu\text{-}H)_2(CO)_{10}]$ (195 mg, 0.23 mmol) and 2-pyridyldimethylsilane (149 mg, 1.08 mmol) were stirred in 15 ml cyclohexane for 72 h. The solution turned from purple to orange whereupon orange precipitate was formed. The orange solid was dissolved in minimum amount of dichloromethane and thin layer chromatograph (tlc) of this solution using a mixture of dichloromethane and hexane (85/15) as the eluant afforded an orange band at $R_f = 0.68$. On recrystallization from dichloromethane, dark orange crystals of **1** were obtained. (Found: C, 25.62, H, 1.92; N, 2.48; Si, 5.29. Calcd. $C_{24}H_{20}N_2O_{10}Si_2Os_3$; C, 25.62; H, 1.97; N, 2.49; Si, 4.99%).

3.3. Synthesis of o-$BrC_6H_4CH_2Si(CH_3)_2H$ (I)

The 2-bromobenzylbromide (100.44 g, 0.40 mol) in dry diethyl ether (*ca.* 200 ml) was added dropwise to magnesium turnings (9.73 g, 0.40 mol) suspended in ether. An ether solution of chlorodimethylsilane (43.63 g, 0.46 mol) was added over 90 min. Saturated aqueous ammonium chloride solution was added slowly until a clear aqueous layer was observed to form below the ether layer. The ether layer was dried overnight with anhydrous sodium sulfate. The ether was then removed under nitrogen. The remaining liquid was subjected to vacuum distillation to yield a colourless liquid over the temperature range 51–56°C at 0.01 mm Hg. Yield: 65% (Found: C, 47.04; H, 5.52; Br, 35.0. Calc. for $C_9H_{13}BrSi$: C, 47.16; H, 5.68; Br, 34.80%).

3.4. Synthesis of 2-$BrC_6H_4CH_2SiCH_3H_2$ (II)

The 2-bromobenzylbromide (40.57 g, 0.16 mol) in dry diethyl ether (*ca.* 200 ml) was added dropwise to magnesium turnings (4.87 g, 0.20 mol) suspended in ether. An ether solution of dichloromethylsilane (31.24 g, 0.27 mol) was added dropwise. A slurry of $LiAlH_4$

was added until no effervescence was observed. The mixture was stirred vigorously for 1 h, after which excess $LiAlH_4$ was destroyed by cautious addition of water. The resultant pale yellow solution was filtered and dried overnight using anhydrous sodium sulfate. The ether was distilled off under nitrogen. Vacuum distillation of the remaining liquid at a pressure of 0.01 mm Hg afforded a colourless liquid at 49–51°C. Yield: 60%. (Found: C, 44.99; H, 5.23; Br, 36.65. Calc. for $C_8H_{11}BrSi$: C, 44.65; H, 5.12; Br, 37.21%).

3.5. Synthesis of o-$BrC_6H_4CH_2SiH_3$

Magnesium turnings (7.31 g, 0.30 mol) were stirred in dry ether, and a few iodine crystals were added. When the colour of iodine had disappeared, 2-bromobenzylbromide (78.62 g, 0.30 mol), dissolved in about 20 ml of dry ether, was introduced dropwise. The reaction mixture was then stirred until most of the magnesium had reacted. The resulting Grignard reagent was transferred to a pressure-equalizing dropping funnel. Trichlorosilane (approximately 50 g, 0.37 mol) was dissolved in dry ether previously cooled to 0°C in a three-necked round-bottom reaction flask. The Grignard reagent was then added dropwise into this solution. When addition was complete, the reaction mixture was stirred for 1 h. Lithium aluminium hydride slurry was added slowly until no effervescence was observed. The reaction mixture was stirred for another hour. Any excess reducing agent was then destroyed by the cautious addition of water. The mixture was filtered under nitrogen, and the pale yellow filtrate was dried with anhydrous sodium sulphate overnight. The ether was removed under nitrogen, and the remaining liquid was distilled under vacuum. A colourless liquid, *o*-bromobenzylsilane, was collected over the temperature range of 43–45°C at a pressure of 0.01 mmHg. Yield: 37% (Found: C, 41.94; H, 4.43; Br, 39.12. Calcd. for C_7H_9BrSi: C, 41.79; H, 4.52; Br, 39.72%).

3.6. Reaction of o-$BrC_6H_4CH_2Si(CH_3)H_2$ with $[Os_3(CO)_{11}(CH_3CN)]$

A CH_2Cl_2 solution of *o*-bromobenzyldimethylsilane (15 mg, 0.07 mmol) was added dropwise to $[Os_3(CO)_{11}(CH_3CN)]$ (30 mg, 0.03 mmol) dissolved in CH_2Cl_2 (20 ml) in a two-necked round-bottom flask fitted with a reflux condenser. A nitrogen inlet connected to the flask provided an inert gas atmosphere. The reaction mixture was stirred for half an hour. After this time, it was found, from thin-layer chromatography of the solution formed, that most of the starting material $[Os_3(CO)_{11}(CH_3CN)]$ had reacted. The concentrated solution was subjected to TLC using dichloromethane/hexane (1.5/8.5) as eluant. **2A** was extracted from the band of $R_f = 0.36$ and recrystallized from a mixture of dichloromethane and hexane. Yield: 95%. (Found: C, 21.67; H, 1.02. Calc. for $C_{20}H_{13}O_{11}BrOs_3Si$: C, 21.67; H, 1.17%).

3.7. Reaction of 2-$BrC_6H_4CH_2Si(CH_3)_2H$ with $[Os_3(CO)_{11}(CH_3CN)]$

A CH_2Cl_2 solution of *o*-bromobenzylmethylsilane (12 mg, 0.06 mmol) was added dropwise to a stirred CH_2Cl_2 solution of $[Os_3(CO)_{11}(CH_3CN)]$ (30 mg, 0.03 mmol) at room temperature for an hour under nitrogen. Thin-layer chromatography of the concentrated solution using dichloromethane/hexane (1.5/8.5) afforded a major product at $R_f = 0.33$ from which **2B** was extracted. **2B** was recrystallized from dichloromethane/hexane. Yield: 100%. (Found: C, 21.29; H, 0.69. Calc. for $C_{19}H_{11}O_{11}BrOs_3Si$: C, 20.85; H, 1.01%).

3.8. Reaction of o-$BrC_6H_4CH_2SiH_3$ with $[Os_3(CO)_{11}(CH_3CN)]$

The $[Os_3(CO)_{11}(CH_3CN)]$ (43 mg, 0.05 mmol) was dissolved in about 20 ml distilled dichloromethane. With stirring and under a nitrogen atmosphere, excess *o*-bromobenzylsilane (20 mg, 0.10 mmol) was added dropwise. The reaction mixture was stirred for one hour. Thin-layer chromatography of the resultant solution showed that most of the starting material, $[Os_3(CO)_{11}(CH_3CN)]$, had reacted. The solution was then evaporated to dryness, leaving an orange residue which was subjected to thin-layer chromatography using as eluant dichloromethane/hexane) (1/4). The major band at $R_f = 0.40$ was yellow in colour. This product was labelled as **2C**, and it was assigned the formula $[Os_3(\mu\text{-H})(CO)_{11}\{2\text{-}BrC_6H_4CH_2SiH_2\}]$, on the basis of its spectral data.

A solution of **2C** in cyclohexane gave the following IR absorptions in the carbonyl region 2133w, 2081ms, 2070w, 2052vs, 2029m, 2015m, 2001s, 1987mw and 1975w cm^{-1}.

The ^1H NMR spectrum of **2C** displayed the following signals: $\delta - 18.930$ (s, Os–H–Os), 2.779 (tr, CH_2), 4.512 (tr, SiH) and 7.229 (m, C_6H_4) ppm. The integral ratio of these signals was found to be approximately 1:2:2:4.

3.9. Reaction of 2-$BrC_6H_4CH_2Si(CH_3)_2H$ with $[Os_3(CO)_{10}(CH_3CN)_2]$

A CH_2Cl_2 solution of 2-bromobenzyldimethylsilane (15 mg, 0.07 mmol) was added dropwise to a CH_2Cl_2 solution of $[Os_3(CO)_{10}(CH_3CN)_2]$ (32 mg, 0.03 mmol) under nitrogen. The reaction mixture was stirred for one hour. The concentrated solution was subjected to TLC using a mixture of dichloromethane/hexane (3/7) as eluant to yield a major band at $R_f = 0.44$ from which orange crystals of **3A**, were obtained upon further recrystallization from hexane. Yield: 98%. (Found: C, 22.71; H, 1.47. Calc. $C_{21}H_{16}NO_{10}BrOs_3Si$: C, 22.49; H, 1.43%).

3.10. Reaction of 2-BrC$_6$H$_4$CH$_2$Si(CH$_3$)H with [Os$_3$(CO)$_{10}$(CH$_3$CN)$_2$]

A CH_2Cl_2 solution of 2-bromobenzylmethylsilane (15 mg, 0.08 mmol) was added dropwise to $[Os_3(CO)_{10}(CH_3CN)_2]$ (31 mg, 0.03 mmol) dissolved in dichloromethane and kept under a nitrogen atmosphere. The resultant solution was stirred for 1 h. TLC of the concentrated solution using a mixture of dichloromethane/hexane (3/7) as the eluant afforded a band at $R_f = 0.30$ from which **3B** was isolated. Yield *ca.* 65%.

3.11. Reaction of o-BrC$_6$H$_4$CH$_2$Si(CH$_3$)$_2$H with [Os$_3$(CO)$_{10}$(CH$_3$CN)$_2$] and P(C$_6$H$_5$)$_3$

Triphenylphosphine (7 mg, 0.02 mmol), dissolved in toluene, was added to a sample of **3A** (25 mg, 0.02 mmol) which was dissolved in a minimum amount of toluene in a reaction tube. The reaction tube was evacuated twice on the vacuum line. The contents of the reaction tube were heated to 40°C for 20 h. An orange-brown residue was obtained upon removal of the solvent. TLC of this reside using a mixture of dichloromethane/hexane (3/7) yielded a major orange band, at $R_f = 0.49$. On recrystallization from a mixture of dichloromethane and hexane, orange crystals of **4** were obtained. Yield: 60%. (Found: C, 33.07; H, 2.05; P, 2.30; Br, 6.44. Calc. $C_{37}H_{28}O_{10}BrOs_3PSi$; C, 33.09; H, 2.09; P, 2.31; Br, 5.96%).

3.12. Reaction of 2-BrC$_6$H$_4$CH$_2$Si(CH$_3$)$_2$H with [Os$_3$(μ-H)$_2$(CO)$_{10}$]

The $[Os_3(\mu\text{-}H)_2(CO)_{10}]$ (50 mg, 0.06 mmol) and 2-bromobenzyldimethylsilane (30 mg, 0.13 mmol), both dissolved in hexane, were allowed to react in an evacuated reaction tube at 60°C for 17 h. Under these conditions, the colour of the solution in the tube turned from purple to yellow. The concentrated solution was subjected to thin-layer chromatography using a mixture of dichloromethane/hexane (1/9) as the eluant to afford a yellow band at $R_f = 0.42$. The product, **5**, appeared to be unstable as it turned from yellow to orange to brown within a few minutes on the silica. Nevertheless, some spectral data of the yellow product were collected, and **5** was tentatively assigned the formula $[Os_3(\mu\text{-}H)_3(CO)_{10}\{o\text{-}BrC_6H_4CH_2Si(CH_3)_2\}]$. The IR spectrum of **5** displays the following absorptions due to carbonyl stretchings: 2126m, 2079s, 2046s, 2034vs, 2009s, 1965m cm^{-1}. The ^1H NMR spectrum consists of the following signals: −12.91 (s, Os–H–Os), −12.60 (s, Os–H–Os), −8.24 (S, Os–H–Os), 0.42 (s, $2CH_3$), 2.62 (s, CH_2) and 7.28 (m, C_6H_4) ppm.

3.13. HPLC separation

The HPLC separations of the osmium clusters were undertaken using a Hewlett-Packard HP1090 liquid chromatograph equipped with a HP-85B personal computer, 3392A integrator and a 1040A diode-array detector. The reversed-phase column (250 × 4 mm internal diameter) used contained LiChrospher 100 CH-18/2, 10 μm. The mobile phase was 100% acetonitrile at a flow rate of 0.5 ml min^{-1}. The temperature in all the runs was 35°C. All solvents were of HPLC grade and were filtered and degassed in helium prior to use. Samples were dissolved in premixed mobile phases filtered through a 0.45 μm pore filter and injected in 5 μl volumes with a Rheodyne model 7010 injector. The column dead volume in each separation was determined with reference to the first baseline peak which appeared on injection.

The identities of all the chromatographic peaks were established as follows: (a) the absorption spectra of the individual osmium clusters were first obtained using a Perkin-Elmer Lambda 9 UV/Vis/NIR spectrophotometer; (b) the absorption spectra of the eluents at specific times corresponding to the peak maxima were determined using the diode-array detector and an evaluation program of the Data Evaluation Pack software of the HP-85B computer, and (c) the resultant spectra were compared with the individual spectra of the compounds, confirming their identities.

The purity of all the observed chromatographic peaks was further checked through (1) overlay of the absorption spectra at three different points (upslope, apex and downslope) of each peak, and (2) determination of the ratio of the heights of the chromatographic peaks monitored at two specific wavelengths (230 and 254 nm). Again, the diode-array detector and the evaluation program (Data Evaluation Pack) of the HP1090 liquid chromatograph were applied. For a pure chromatographic peak the spectral overlay should match, and the ratio of the two signals across a peak elution profile should remain fairly constant. Using these methods, many of the chromatographic peaks obtained from the separations were found to correspond to pure triosmium cluster compounds.

References

1 (a) H.G. Ang, B. Chang and W.L. Kwik, *J. Chem. Soc., Dalton Trans.*, (1992) 2161; (b) H.G. Ang and W.L. Kwik, *J. Organomet. Chem.*, *361* (1989) 27.

2 (a) A.J. Deeming and R. Peters, *J. Chem. Soc., Dalton Trans.*, (1982) 1205; (b) K. Burgess, D. Holden, B.F.G. Johnson and J. Lewis, *J. Chem. Soc., Dalton Trans.* (1985) 85; (c) A. Eisenstadt,

C.M. Giandomencio, M.F. Frederick and R.M. Laine, *Organometallics*, *4* (1985) 2033; (d) R. Zoet, G. Van Koten, K. Vrieze, J. Jansen, K. Goubilz and C.H. Stam, *Organometallics*, *7* (1988) 1565.
3 (a) C. Eaborn, *Organosilicon compounds*, Butterworths, London, 1960; (b) W.G. Brown, in R. Adams (ed.), *Organic Reactions*, Vol VI, Wiley, New York, 1960.
4 R.N. Kniseley, V.A. Fassel and E.E. Conrad, *Spectrochim. Acta*, *15* (1959) 651.
5 E.A. Williams, in S. Patar and Z. Rappoport (eds), *The Chemistry of Organic Silicon Compounds*, Wiley, New York, 1989.
6 B.F.G. Johnson, J. Lewis, M. Monari, D. Braga, F. Grepioni and C. Gradella, *J. Chem. Soc., Dalton Trans.*, (1990) 2863.
7 R.D. Adams, J.E. Cortopassi and M.P. Pompeo, *Inorg. Chem.*, *30* (1991) 2960.
8 G.N. van Buuren, A.C. Willis, F.W.B. Einstein, L.K. Peterson, R.K. Pomeroy and D. Sutton, *Inorg. Chem.*, *20* (1981) 4361.
9 A.C. Willis, F.W.B. Einstein, R.M. Ramadan and R.K. Pomeroy, *Organometallics*, *2* (1983) 935.
10 F.W.B. Einstein, R.K. Pomeroy and A.C. Willis, *J. Organomet. Chem.*, *311* (1986) 257.
11 K. Burgess, B.F.G. Johnson and J. Lewis, *J. Organomet. Chem.*, *233* (1982) C55.
12 B.F.G. Johnson, J. Lewis and M. Monari, *J. Chem. Soc., Dalton Trans.*, (1990) 3525.
13 A.P. Humphries and H.D. Kaesz, *Prog. Inorg. Chem.*, *25* (1979) 145.
14 M.R. Churchill and B.G. DeBoer, *Inorg. Chem.*, *16* (1977) 878.
15 A.J. Deeming, S. Donovan-Mtunzi, K.I. Hardcastle, S.E. Kabir, K. Henrick and M. McPartlin, *J. Chem. Soc., Dalton Trans.*, (1988) 579.
16 P.A. Dawson, B.F.G. Johnson, J. Lewis, J. Puga, P.R. Raithby and M.J. Rosalles, *J. Chem. Soc., Dalton Trans.*, (1982) 233.
17 A.C. Willis, G.N. van Buuren, R.K. Pomeroy and F.W.B. Einstein, *Inorg. Chem.*, *22* (1983) 1162.
18 B.L. Karger, L.R. Snyder and C. Horrain, *An Introduction to Separation Science*, Wiley, New York, 1973.
19 V.B. Meyer, *J. Chromatogr.*, *334* (1985) 197.
20 H.G. Ang, W.L. Kwik and W.K. Leong, *J. Organomet. Chem.*, *379* (1989) 325.
21 H.G. Ang, W.L. Kwik and E. Morrison, *J. Fluorine Chem.*, *51* (1991) 83.
22 H.G. Ang, W.L. Kwik and W.K. Leong, *J. Chromatogr.*, *537* (1991) 475.
23 L.R. Snyder and J.J. Kirkland, *Introduction to Modern Liquid Chromatography*, 2nd Ed., Wiley, New York, 1979.
24 A. Mangia, G. Predieu and E. Sappa, *Anal. Chim Acta*, *152* (1983) 289.
25 A. Casoli, A. Mangia, G. Predieu and E. Sappa, *Anal. Chim. Acta*, *176* (1985) 259.
26 A. Casoli, A. Mangia, G. Predieu and E. Sappa, *J. Chromatogr.*, *447* (1988) 187.
27 G.M. Sheldrick, Siemens, Madison, WI, 1986.